ELSEVIER

Journal of Hazardous Materials B 63 (1998) 69–90

Journal of Hazardous Materials

Decomposition of methyl chloride by using an RF plasma reactor

Lien-Te Hsieh [a,*], Wen-Jhy Lee [a], Chuh-Yung Chen [b], Yo-Ping Greg Wu [c], Shui-Jen Chen [d], Ya-Fen Wang [a]

[a] *Department of Environmental Engineering, National Cheng Kung University, Tainan 70101, Taiwan*
[b] *Department of Chemical Engineering, National Cheng Kung University, Tainan 70101, Taiwan*
[c] *Department of Chemical Engineering, National I-Lan Institute of Technology, I-Lan 26011, Taiwan*
[d] *Department of Environmental Engineering and Science, National Ping-Tung University of Science and Technology, Nei Pu 91207, Ping Tung, Taiwan*

Received 24 February 1998; revised 4 July 1998; accepted 13 July 1998

Abstract

Application of radio-frequency (RF) plasma as an alternative technology for the decomposition of methyl chloride (CH_3Cl) with oxygen is demonstrated. The results of this study revealed that, in the $CH_3Cl/O_2/Ar$ plasma, the decomposition fraction of CH_3Cl was over 99.99%, which occurred at the condition designed for 3% of CH_3Cl feeding concentration, 1.0 of equivalence ratio (ϕ), 20 Torr of operation pressure, 100 sccm of total gas flow rate and 100 W of input power wattage. Higher input power wattage can increase both the CH_3Cl decomposition efficiency and the fraction of total-carbon input converted into $[CO_2 + CO]$, resulting in the reduction of the harmful products ($COCl_2$) effluent concentration. However, more soot was found in the plasma reactor when the input power wattage was higher than 70 W. The species detected in the effluent gas stream included CO, CO_2, H_2O, HCl, CH_4, C_2H_2, C_2H_4, C_2H_6, C_2H_3Cl, C_2H_5Cl and $COCl_2$. The optimal mathematical models based on obtained experimental data were also developed and tested by means of the sensitivity analysis, which showed that the input power wattage (W) was the most sensitive parameter for both CH_3Cl decomposition and temperature elevation in the RF plasma reactor.

Keywords: Radio-Frequency (RF); Plasma; Methyl chloride; Decomposition; Sensitivity analysis

* Corresponding author. Tel.: +886 6 2757575, ext. 54531; fax: +886 6 2752790.

0304-3894/98/$ - see front matter
PII: S0304-3894(98)00182-4

1. Introduction

Over the last two decades, interest in the study of safe destruction technologies for chlorinated hydrocarbons (CHCs) or clorofluorocarbons (CFCs) has greatly increased. In the early years, many research and development were mainly focused on various decomposition technologies involving incineration [1–3], pyrolysis [4,5], catalyst [6,7], chemical reaction [8–10], UV irradiation [11,12], and so on. Recently, a lot of alternative thermal and non-thermal plasma technologies have been developed [13,14]. Barat and Bozzelli have studied the destruction of halogenated hydrocarbons in low-pressure tubular reactors using microwave discharges [15]. Yamamoto et al. have showed that a greater than 95% decomposition of Halon FC-12B ($CClBrF_2$) was achieved with dry air in a bench-scale pulsed corona reactor [16]. Cleland and Hess have demonstrated the decomposition of N_2O in a 13.56 MHz parallel-plate plasma system, analyzed by using in situ Fourier transform infrared (FTIR) spectroscopy [17]. Arno et al. have investigated the characterization of surface wave plasmas and their application to the detoxification of high concentrations of acetone [18]. In addition, the application of surface wave plasma as an alternative technology for the destruction and removal of trichloroethylene pollutants has been described [19].

With the characteristics of high electrical and thermal conductivity, the plasma flame can provide an excellent energy conversion and heat transfer medium for reactants and products. Consequently, the energy utilization efficiency of 80–90% in plasma furnaces is higher than in many other furnaces/incinerators [20]. The temperature of the gas molecule in an RF plasma reactor is near room temperature, while the temperature of electrons will be higher than 10^4 K. At such high temperature, the energy of an electron is much higher than 50 kcal/mol. It is two times of magnitude higher than the activation energy of a conventional chemical reaction (25 kcal/mol). Therefore, the conventional reaction which needs to proceed at a very high temperature will be finished at a lower temperature in the RF plasma reactor [21–23]. Besides, unlike DC plasma, RF plasma is free from electrode erosion or corrosion caused by the reactive gases such as hydrogen chloride and hydrogen fluoride which occur during CHCs or CFCs decomposition.

In this study, the decomposition of methyl chloride in the RF plasma environment was investigated. The reasons are as following: (1) Methyl chloride is the simplest chloro-hydrocarbon and as such plays a fundamental role in our understanding of more complex chlorinated hydrocarbons; (2) despite the efforts and progress in the former, a comprehensive and detailed decomposition of methyl chloride in the RF plasma is still lacking. (3) Methyl chloride is an abundant environmental mutagen and carcinogen. Since methyl chloride is used in the chemical industry as a methylating agent, the consequences of occupational exposure have received much attention initiating investigations into its toxicity and metabolism [24]. Therefore, an RF plasma reactor for methyl chloride decomposition is of great interest. The effect of plasma operational-parameters for the methyl chloride decomposition, the effluent species, and the carbon balance were investigated. In addition, the mathematical models established from the regression analyses of experimental data was obtained and the sensitivity analyses for these models were also investigated.

2. Experimental section

Our plasma system (see Fig. 1) is the same to our previous studies and is described in more detail in [22]. The main components of the experimental equipment include a vacuum pump, a gas introduction device (mass flow controllers), an RF power, an excitation source producing electromagnetic radiation within radio frequencies for initiating and sustaining plasma and a Fourier Transform Infrared Spectrometer (FTIR) analysis system.

This RF plasma reactor is a cylindrical glass vessel which has a diameter of 4.14 cm and a height of 15 cm. The outer copper electrode has a height of 5.4 cm and is wrapped on the plasma reactor and grounded. A plasma generator (PFG 600 RF, Fritz Huttinger Elektronik) and a matching network (Matchbox PFM) supply 13.56 MHz RF power to the outer copper electrode. Gas introduced into the bottom of the reactor flows through glass tubes where it mixes before flowing into the copper electrode zone. This arrangement ensures that all gas introduced into the reactor flows through the glow discharge.

For each designed operational condition, the feeding concentration of gas (including reactants gas, auxiliary gas, and carrier gas), the operational pressure, the gas flow rate, and the input power wattage were measured more than three times within 5 min in order to assure that steady state conditions were achieved.

The introduction of gas flows was controlled by mass flow controllers, obtained from Tylan, USA. The reactor was evacuated through the center of the reactor at low pressure (controlled at 20 Torr). This arrangement ensured radially symmetric flow profiles which helped minimize radial concentration gradients between the glow discharge and the glass walls. The gaseous product species out of the reactor was on-line introduced

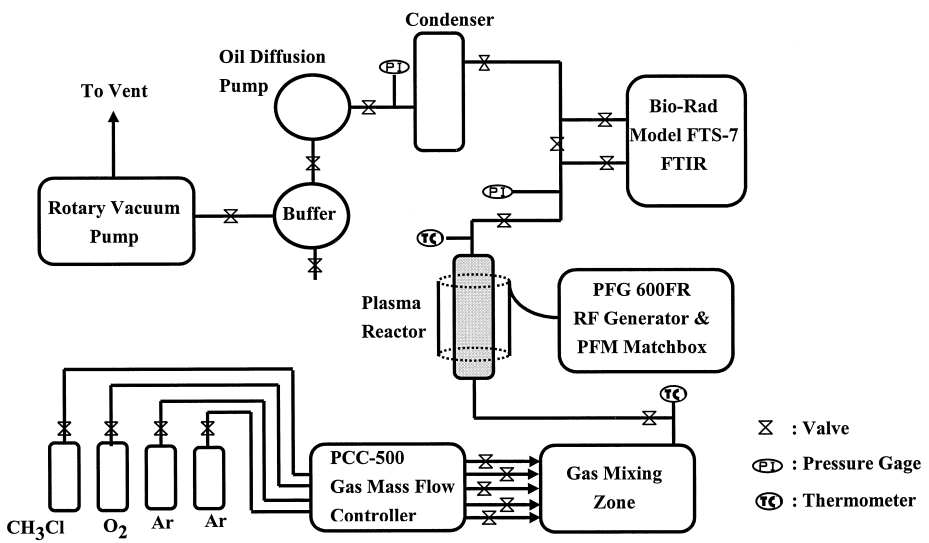

Fig. 1. Scheme of plasma system.

into a Fourier transform infrared (FTIR) spectrometer (Bio-Rad, Model FTS-7) for species identification and quantification. After the pressure of the plasma system fell below 1 Torr, a diffusion pumped system trapped with liquid oil was used to keep the system pressure lower than 10^{-3} Torr for the clean-up of contamination. Calibration of standard gaseous reactants and product species was done by withdrawing unreacted gases and by going directly through the sampling line connected to the FTIR. The mass of species was calculated by comparing the response factor (absorbance height/concentration) of standard gas at the same Infrared Spectrometer (IR) wave number. The wave numbers of both absorbance-zone range and -peak center for CO_2, CO, CH_4, C_2H_6, C_2H_4, C_2H_2, H_2O, CH_3Cl, C_2H_3Cl, C_2H_5Cl, and $COCl_2$ were obtained from the previous studies [21–23,25], identified and quantified in this study. In order to make sure that the experimental results are reproducible, all of the experiments were repeated at least three times and the averaged data are presented. In order to understand the significance of deposition and condensation that occurred in the sampling and analyzing system, the FTIR quantification data were also checked through carbon-balances.

3. Results and discussion

A steady-state was considered to be reached when relatively constant values of both decomposition fractions and the absorbance-peaks of product species on FTIR were obtained at designed operational parameters (namely, feeding concentration of methyl chloride C_{CH3Cl}; operational pressures P; total gas flow rate Q; input power wattage W; and equivalence ratio $\phi = [in_{CH3Cl}/in_{O2}]_{actual} \times [in_{O2}/in_{CH3Cl}]_{stoichiometric}$). Each run of experiment lasted for 40 min and the effluent concentration of individual species was monitored by the FTIR from the start time of reaction to 40 min. In all experiments, the results show the steady-state of effluent concentration were reached after 20 min. It should be noted that data reported herein are based on the mean values measured after a steady-state condition had been reached.

3.1. Decomposition of CH_3Cl in the RF plasma reactor

The decomposition fraction (%) of CH_3Cl, η_{CH3Cl}, is defined as follows:

$$\eta_{CH3Cl} = \left[(C_{in} - C_{out})/(C_{in})\right] \times 100\% \quad (1)$$

where C_{in} = the feeding concentration of CH_3Cl (%); C_{out} = the effluent concentration of CH_3Cl (%).

The η_{CH3Cl} can be used to further assess the performance of different operational conditions.

Experiments were carried out for the determination of η_{CH3Cl} in $CH_3Cl/O_2/Ar$ plasma under the following condition: argon was used as a carrier gas; operational pressure was controlled at 20 Torr; the total flow rate was 100 sccm; and the input power wattages were varied as 50, 70, 90, and 100 W, respectively. At three different CH_3Cl feeding concentrations (3%, 5%, and 10.7%), the equivalence ratio ϕ varied from 0.5 to 2.0.

At both 90 and 100 W of input power wattage, the η_{CH3Cl} was between 99.36% and 99.99%, and there was found to be no significant difference from varying a ϕ value

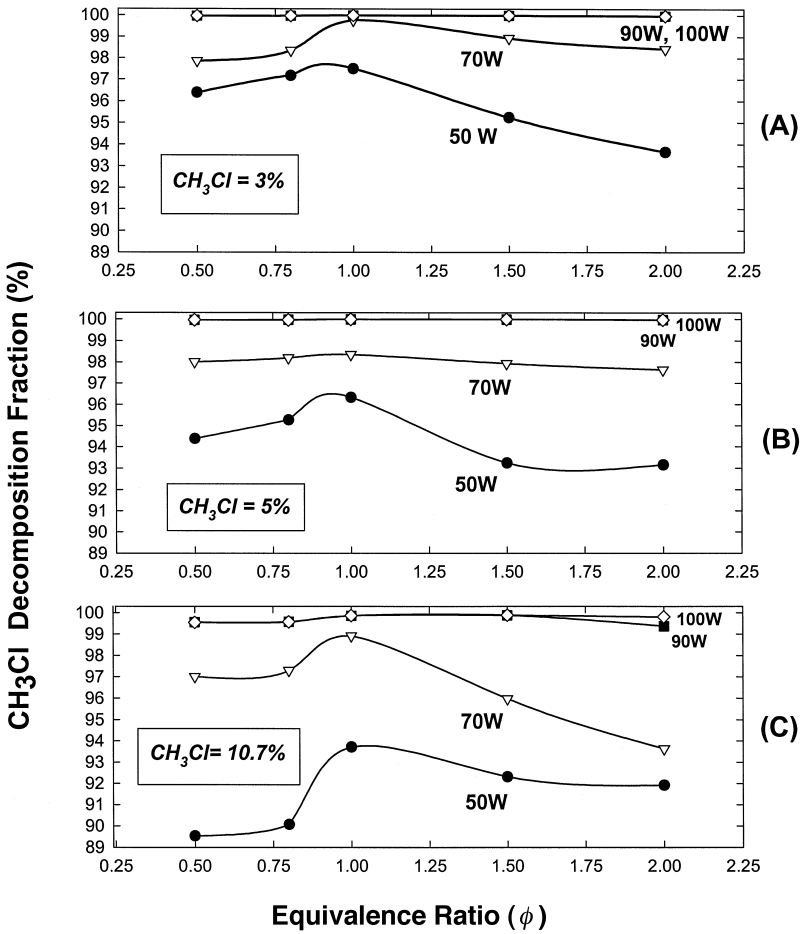

Fig. 2. CH_3Cl decomposition fraction (%) vs. equivalence ratio (ϕ) under the condition of different input power wattage.

from 0.5 to 2.0 (Fig. 2A ~ C). When higher input power wattage was applied, the energy transfer efficiency of both Ar plasma and O_2 in the plasma reactor was higher than that in lower input power case. This condition resulted in the increasing of effective collision frequency among the reactants, excited Ar ($Ar*$) and free electron (e^-), and therefore, elevated the CH_3Cl decomposition efficiency.

At both 50 and 70 W, the η_{CH3Cl} were between 89.53% and 97.50% and between 93.63% and 98.93%, respectively (Fig. 2A ~ C). The CH_3Cl decomposition fraction (%) was increased at a ϕ value between 0.5 and 1.0 and decreased when the ϕ value was between 1.0 and 2.0. This result indicates that higher ϕ value ($\phi > 1$) provides less oxygen and reduces the possibility of CH_3Cl oxidation. However, when the ϕ value decreased from 1.0 to 0.5, in the reactor, the concentration ratio of Ar/O_2 was decreased very significantly. This is due to the fact that the energy transfer efficiency of

Ar is much higher than that of O_2 [21] and results in a higher decomposition fraction of CH_3Cl.

In this $CH_3Cl/O_2/Ar$ plasma, the η_{CH3Cl} averaged 99.88% at both 90 and 100 W, 97.75% at 70 W and 93.99% at 50 W, respectively. Elevating the input power wattage significantly enhanced the decomposition fraction of CH_3Cl.

It is important to describe the reaction mechanism by taking the whole system into consideration. This is because the basic parameters like the compounds used (CH_3Cl,

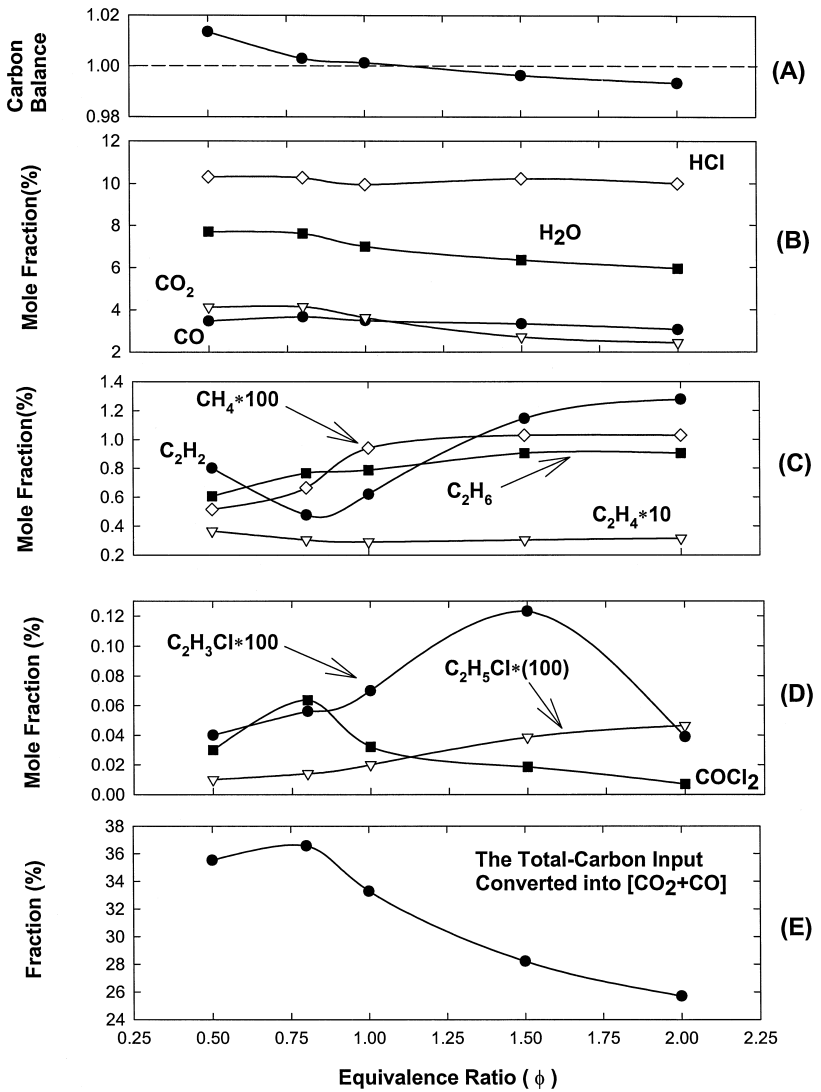

Fig. 3. The effect of equivalence ratio for carbon balance (A), effluent concentration of products (B ~ D), and the fraction of total-carbon converted into CO_2 and CO (E).

O_2, Ar), and the activation is the same in all experiments. When input power wattage is adequate, the initiating free radicals can be done by the following reactions.

$$\text{Energy} + \text{Ar} \rightarrow \text{Ar}* \quad (2)$$

$$CH_3Cl + \text{Ar}* \rightarrow CH_3^{\cdot} + Cl^{\cdot} + \text{Ar} \quad (3)$$

$$\rightarrow CH_2Cl^{\cdot} + HCl + \text{Ar} \quad (4)$$

$$\rightarrow \text{other reactions} \quad (5)$$

The major pathways for CH_3Cl decomposition include $CH_3Cl + \text{Ar}* \rightarrow CH_3^{\cdot} + Cl^{\cdot} + \text{Ar}$, $CH_3Cl + (O^{\cdot}, Cl^{\cdot}, OH^{\cdot}) \rightarrow CH_2Cl^{\cdot} + (OH^{\cdot}, HCl, H_2O)$ and its unimolecular decomposition $CH_3Cl \rightarrow CH_3^{\cdot} + Cl^{\cdot}$. This will be discussed further below.

3.2. Effect of the equivalence ratios

Several experiments were conducted for insight into the effect of varying equivalence ratio for carbon balance, effluent concentration of products, and the fraction of total-carbon converted into $[CO_2 + CO]$. The operational parameters were designed as following: argon was used as the carrier gas; the equivalence ratio (ϕ) was varied from 0.5 to 2.0; the feeding concentration of CH_3Cl feeding concentration was 10.7%; the operational pressure was controlled at 20 Torr; the total gas flow rate was 100 sccm; and input power wattage was 50 W.

The presence of oxygen in a certain range can accelerate the rate of CH_3Cl decomposition because the reaction $OH^{\cdot} + HCl = H_2O + Cl^{\cdot}$ reliberates the $Cl^{\cdot}$ radical. The other important reaction, $CH_3Cl + O_2 = CH_2Cl^{\cdot} + HO_2^{\cdot}$, also contributes to the rate of CH_3Cl consumption [5].

At a ϕ value greater than 1.25, the value of carbon balance was lower than 1.0. This was due to more soot formation in the plasma reactor (Fig. 3A).

CH_4 is an inevitable byproduct of CH_3Cl decomposition. HCl rapidly converts the $CH_3^{\cdot}$ radicals into CH_4 by $CH_3^{\cdot} + HCl = CH_4 + Cl^{\cdot}$ and contributes to the major formation of CH_4 [5].

The effluent concentration of CH_4 was also increased at a ϕ value between 0.5 and 1.0 and at the same level with in a ϕ value between 1.0 and 2.0 (Fig. 3C). At a higher equivalence ratio (ϕ), the decomposition of CH_4 into small radicals, such as $CH_3^{\cdot}$, $CH_2^{\cdot}$ and $CH^{\cdot}$ is very significant. The major reactions are as follows [5,22,25].

$$CH_4 + e^- \rightarrow CH_3^{\cdot} + H^{\cdot} + e^- \quad (6)$$

$$CH_3^{\cdot} + e^- \rightarrow CH_2^{\cdot} + H^{\cdot} + e^- \quad (7)$$

$$CH_2^{\cdot} + e^- \rightarrow CH^{\cdot} + H^{\cdot} + e^- \quad (8)$$

$$CH_4 + \text{Ar}* \rightarrow CH_3^{\cdot} + H^{\cdot} + \text{Ar} \quad (9)$$

$$CH_3^{\cdot} + \text{Ar}* \rightarrow CH_2^{\cdot} + H^{\cdot} + \text{Ar} \quad (10)$$

$$CH_2^{\cdot} + \text{Ar}* \rightarrow CH^{\cdot} + H^{\cdot} + \text{Ar} \quad (11)$$

$$CH_4 + H^{\cdot} \rightarrow CH_3^{\cdot} + H_2 \quad (12)$$

$$CH_3^{\cdot} + O_2 \rightarrow CH_3O^{\cdot} + O^{\cdot} \quad (13)$$

$$CH_3^{\cdot} + O_2 \rightarrow CH_2O + OH^{\cdot} \quad (14)$$

$$CH_3^{\cdot} + O^{\cdot} \rightarrow CH_2O + H^{\cdot} \quad (15)$$

$$CH_3^{\cdot} + OH^{\cdot} \rightarrow CH_3O^{\cdot} + H^{\cdot} \quad (16)$$

$$CH_3^{\cdot} + OH^{\cdot} \rightarrow CH_2O + H_2 \quad (17)$$

$$CH_2^{\cdot} + O_2 \rightarrow CO_2 + H^{\cdot} + H^{\cdot} \quad (18)$$

$$CH_2^{\cdot} + O_2 \rightarrow CH_2O + O^{\cdot} \quad (19)$$

$$CH_2^{\cdot} + O_2 \rightarrow CO_2 + H^{\cdot} + H^{\cdot} \quad (20)$$

$$CH_2^{\cdot} + O^{\cdot} \rightarrow CO^{\cdot} + H^{\cdot} + H^{\cdot} \quad (21)$$

The effluent concentration of C_2H_4 showed no significant variation at a ϕ value between 0.5 and 2.0. This means that both formation and decomposition of C_2H_4 occurred dynamically in the $CH_3Cl/O_2/Ar$ plasma. The recombination of $CH_2^{\cdot}$ and $CH_2^{\cdot}$ results in formation of C_2H_4. The decomposition of C_2H_6 and $C_2H_5^{\cdot}$ also results in formation of C_2H_4. That is,

$$CH_2^{\cdot} + CH_2^{\cdot} \rightarrow C_2H_4 \quad (22)$$

$$CH^{\cdot} + CH_3^{\cdot} \rightarrow C_2H_4 \quad (23)$$

$$CH_3^{\cdot} + CH_3^{\cdot} \rightarrow [C_2H_6]* \rightarrow C_2H_4 + H_2 \quad (24)$$

$$CH_2^{\cdot} + CH_3^{\cdot} \rightarrow C_2H_5^{\cdot} \quad (25)$$

$$C_2H_5^{\cdot} \rightarrow C_2H_4 + H^{\cdot} \quad (26)$$

$$C_2H_4 + H^{\cdot} \rightarrow C_2H_3^{\cdot} + H_2 \quad (27)$$

In the proposed mechanism, CO forms primarily via $CHO^{\cdot} + M = CO + H^{\cdot} + M$ and to a lesser extent via $CHO^{\cdot} + O_2 = CO + HO_2^{\cdot}$ [5]. The major path for the formation of $CHO^{\cdot}$ occurs via $C_2H_3^{\cdot} + O_2 = CH_2O + CHO^{\cdot}$. The CH_2O formed is also rapidly decomposed into $CHO^{\cdot}$ by the reaction

$$CH_2O + Cl^{\cdot} = CHO^{\cdot} + HCl \quad (28)$$

In Fig. 3C, the concentration of C_2H_6 was slightly increased at a ϕ value between 0.5 and 1.5 and leveled off at a ϕ value higher than 1.5. At a higher equivalence ratio (ϕ) the decomposition of C_2H_6 into small species like $CH_3^{\cdot}$ and $C_2H_5^{\cdot}$ radicals is significant. The reactions are as follows.

$$CH_3^{\cdot} + CH_3^{\cdot} \rightarrow C_2H_6 \quad (29)$$

$$C_2H_5^{\cdot} + H^{\cdot} \rightarrow C_2H_6 \quad (30)$$

$$C_2H_6 + H* \rightarrow C_2H_5^{\cdot} + H_2 \quad (31)$$

The effluent concentration of C_2H_2 was decreased at a ϕ value between 0.5 and 0.75, but increased at a ϕ value between 0.75 and 1.5. This probably can be explained

by the fact that the formation reaction of C_2H_2 is dominant at a ϕ value between 0.75 and 1.5 (Fig. 3C). The formation of C_2H_2 can be shown by the following reactions.

$$CH^{\cdot} + CH^{\cdot} \rightarrow C_2H_2 \quad (32)$$

$$CH_2^{\cdot} + CH^{\cdot} \rightarrow C_2H_2 + H^{\cdot} \quad (33)$$

$$C_2H_3^{\cdot} + H^{\cdot} \rightarrow C_2H_2 + H_2 \quad (34)$$

$$C_2H_3^{\cdot} + O_2 \rightarrow C_2H_2 + HO_2^{\cdot} \quad (35)$$

$$C_2H_4 + H^{\cdot} \rightarrow C_2H_3^{\cdot} + H_2 \rightarrow C_2H_2 + H_2 \quad (36)$$

$$C_2H_3^{\cdot} + Ar* \rightarrow C_2H_2 + H^{\cdot} + Ar* \quad (37)$$

$$C_2H_3Cl \rightarrow C_2H_2 + HCl \quad (38)$$

Reactions from (34) to (38) are primarily responsible for the formation of C_2H_2 in the RF plasma reactor.

At a ϕ value between 0.5 and 0.75, the formation of C_2H_2 was hindered due to the competition of the formation of other saturated or unsaturated C_2 species. Fig. 3C shows that a measured minimum concentration of C_2H_2 occurred at $\phi = 0.75$ in this investigation. However, C_2H_2 is a moderately stable compound in the effluent mixture.

A C_2H_3Cl concentration is increased at a ϕ value between 0.5 and 1.5 and decreased when the ϕ value is between 1.5 and 2.0 (Fig. 3D). This can be explained by the fact that the decomposition fraction of CH_3Cl is hindered more significantly at an equivalence ratio between 1.5 and 2.0 and provides a lesser amount of $CH_2Cl^{\cdot}$ and $CHCl^{\cdot}$ radicals to form C_2H_3Cl. The CH_3Cl decomposition is mostly by self-dissociation or through attack by the e^-, $O^{\cdot}$, $Cl^{\cdot}$, $OH^{\cdot}$ or $CH_3^{\cdot}$. Those reaction were as follows [5,25].

$$CH_3Cl + M = CH_3^{\cdot} + Cl^{\cdot} + M \quad (39)$$

$$CH_3Cl + M = CH_2Cl^{\cdot} + H^{\cdot} + M \quad (40)$$

$$CH_3Cl + (O^{\cdot},Cl^{\cdot},OH^{\cdot}) = CH_3Cl* + (O^{\cdot},Cl^{\cdot},OH^{\cdot}) \quad (41)$$

$$CH_3Cl* + (O^{\cdot},Cl^{\cdot},OH^{\cdot}) = CH_2Cl^{\cdot} + (OH^{\cdot},HCl,H_2O) \quad (42)$$

$$CH_2Cl^{\cdot} + (O^{\cdot},Cl^{\cdot},OH^{\cdot}) = CHCl^{\cdot} + (OH^{\cdot},HCl,H_2O) \quad (43)$$

$$CH_3Cl + H^{\cdot} = CH_3^{\cdot} + HCl \quad (44)$$

$$CH_3Cl + CH_3^{\cdot} = CH_3Cl* + CH_3^{\cdot} \quad (45)$$

Reactions (39) ~ (42) and (44) are primarily responsible for the decomposition of CH_3Cl in the RF plasma reactor.

Both $CH_2Cl^{\cdot}$ and $CHCl^{\cdot}$ are the important radicals for further production of C_2H_3Cl. The formation of low levels of C_2H_3Cl can be represented by the following two reactions [25].

$$CH_2Cl^{\cdot} + CHCl^{\cdot} = [CH_2ClCHCl]* = C_2H_3Cl + Cl^{\cdot} \quad (46)$$

$$CH_2Cl^{\cdot} + CH_2Cl^{\cdot} = [CH_2ClCH_2Cl]* = C_2H_3Cl + HCl \quad (47)$$

Vinyl chloride (C_2H_3Cl) is the important precursor for acetylene, and is produced via the chemically activated recombination of $CH_2Cl^{\cdot}$ radicals [5]. At a higher equivalence

ratio (ϕ), the levels of both $CH_2Cl^{\cdot}$ and $CHCl^{\cdot}$ decrease in the plasma reactor, and therefore, the formation of C_2H_3Cl is hindered.

The effluent concentration of C_2H_5Cl was increased by increasing the equivalence ratio (Fig. 3D). The formation of low levels of C_2H_5Cl can be explained by the following reactions [25].

$$C_2H_6 + Cl^{\cdot} = C_2H_5^{\cdot} + HCl = C_2H_5Cl + H^{\cdot} \quad (48)$$

$$C_2H_6 + Cl_2 = C_2H_5Cl + HCl. \quad (49)$$

At a higher equivalence ratio (ϕ), the concentration of C_2H_6 was higher, and therefore, enhanced the production of C_2H_5Cl. In the plasma reactor, the formation of C_2H_5Cl also resulted from the collision of $CH_2Cl^{\cdot}$ and $CH_3^{\cdot}$ radicals, by the reaction 50 [25].

$$CH_2Cl^{\cdot} + CH_3^{\cdot} = [CH_3CH_2Cl]* = C_2H_5Cl. \quad (50)$$

Because $CH_2Cl^{\cdot}$ is an important radical for the formation of both C_2H_5Cl and C_2H_3Cl, the formation of C_2H_5Cl was primarily under the influence of the level of C_2H_6. This caused the trend of C_2H_5Cl to be similar to that of C_2H_6 in the effluent gas stream. However, both C_2H_3Cl and C_2H_5Cl concentrations are much lower than those hydrocarbon species shown in Fig. 3C.

A $COCl_2$ concentration is increased at a ϕ value between 0.5 and 0.8 and decreased when the ϕ value is between 0.8 and 2.0 (Fig. 3D). In this plasma reactor, $COCl_2$ was formed from the combination of CO or $COCl^{\cdot}$ with $Cl^{\cdot}$ by the following reactions [23,25].

$$CO + Cl^{\cdot} = COCl^{\cdot} \quad (51)$$

$$CO + Cl_2 + Ar* = COCl^{\cdot} + Cl^{\cdot} + Ar \quad (52)$$

$$COCl^{\cdot} + Cl^{\cdot} = COCl_2. \quad (53)$$

In addition, the reaction of CO and Cl_2 occurs in the excited plasma reactor:

$$CO + Cl_2 = COCl_2. \quad (54)$$

Besides the atom C and Cl, the formation of more $COCl_2$ also needs more oxygen supply. With the increase of equivalence ratio (ϕ) from 1.0 to 2.0, the reduction in oxygen feeding concentration hindered CH_3Cl oxidation and reduced the possibility of both CO_2 and CO formation. Thus, this condition resulted in less $COCl_2$ formation. At a ϕ value between 0.5 and 1.0, although the feeding concentration of oxygen is higher and resulted in more $COCl_2$ formation, the possibility of $COCl_2$ decomposition was also higher. $COCl_2$ was easily attacked by both $Cl\cdot$ and $H\cdot$ radicals and decomposed by the following reactions [23,25]:

$$COCl_2 + (Cl^{\cdot}, H^{\cdot}) = COCl^{\cdot} + (Cl_2, HCl) \quad (55)$$

$$COCl^{\cdot} + M = CO + Cl^{\cdot} + M \quad (56)$$

$$COCl_2 + M = CO + Cl_2 + M. \quad (57)$$

Thus, the maximum effluent concentration of $COCl_2$ appeared at $\phi = 0.8$ in this investigation (Fig. 3D).

The destruction and removal efficiency (DRE) of chlorinated hydrocarbons (CHCs) expressed only by the reactant disappearance fraction was not satisfied for practical

applications. The additional parameter was the $[CO_2 + CO]$ conversion fraction (%), which was defined as the fraction (%) of total carbon input converted into CO_2 and CO [21]. Fig. 3E shows that when the equivalence ratio (ϕ) increased from 0.5 to 2.0, the fraction of total-carbon input converted into $[CO_2 + CO]$ decreased from 36.6% to 25.7%. A lower oxygen feeding concentration hindered CH_3Cl oxidation and reduced the possibility of both CO_2 and CO formation. The fact that parts of carbon was converted into soot also contributed to decreasing of the fraction of total-carbon input converted into $[CO_2 + CO]$. This tendency revealed that higher (ϕ) value represents less oxygen concentration resulting in less total carbon converted into $[CO_2 + CO]$.

3.3. Effect of input power wattage

Several experiments were also conducted for insight into the effect of varying input power wattage for carbon balance, effluent concentration of products, and the fraction of total-carbon converted into CO_2 and CO. The operational parameters were designed as the following: argon was used as the carrier gas; input power wattages were varied from 50 to 100 W; the CH_3Cl feeding concentration was 10.7%; the operational pressure was controlled at 20 Torr; the total gas flow rate was 100 sccm; and the equivalence ratio (ϕ) was 1.0.

At higher input power wattages, more soot formation and polymerization were found in the plasma reactor. This resulted in a lower carbon balance in the effluent gas stream (Fig. 4A).

In Fig. 4B, the effluent concentrations of HCl, H_2O, and CO_2 were increased by increasing the input power wattage. This can be explained by the fact that higher input power wattage provided more energy in the plasma reactor and made the reaction more complete. Therefore, the effluent concentration of HCl, H_2O and CO_2 were higher at a higher input power wattage.

The effluent concentration of CO was also increased by increasing the input power wattage from 50 to 70 W, but leveled off at 90 and 100 W (see Fig. 4B). This is due to the fact that higher input power wattage will enforce the CO converted into CO_2 by the reaction:

$$CO + OH^{\cdot} = CO_2 + H^{\cdot}. \quad (58)$$

Moreover, CO_2 is more stable than CO. Therefore, the effluent concentration of CO is lower than that of CO_2 with an increase of the input power wattage from 60 to 100 W.

In Fig. 4C, the mole fraction profiles for CH_4, C_2H_2, C_2H_4, and C_2H_6 are presented for different input power wattages. Generally, increases in input power wattage decreased the levels of CH_4, C_2H_2, C_2H_4, and C_2H_6. The species of CH_4,C_2H_2, and C_2H_4 were not found when the input power wattages were higher than 70, 90, and 100 W, respectively. These results revealed that, at higher ϕ values, more hydrocarbons (CH_4, C_2H_2, C_2H_4 and C_2H_6) not only converted into CO_2 and CO, but also formed soot.

In Fig. 4D, almost all the effluent concentrations were lower at a higher input power wattage. The reduction of C_2H_3Cl and C_2H_5Cl also exhibited a trend similar to those hydrocarbon species shown in Fig. 4C. There was no C_2H_3Cl and C_2H_5Cl formation

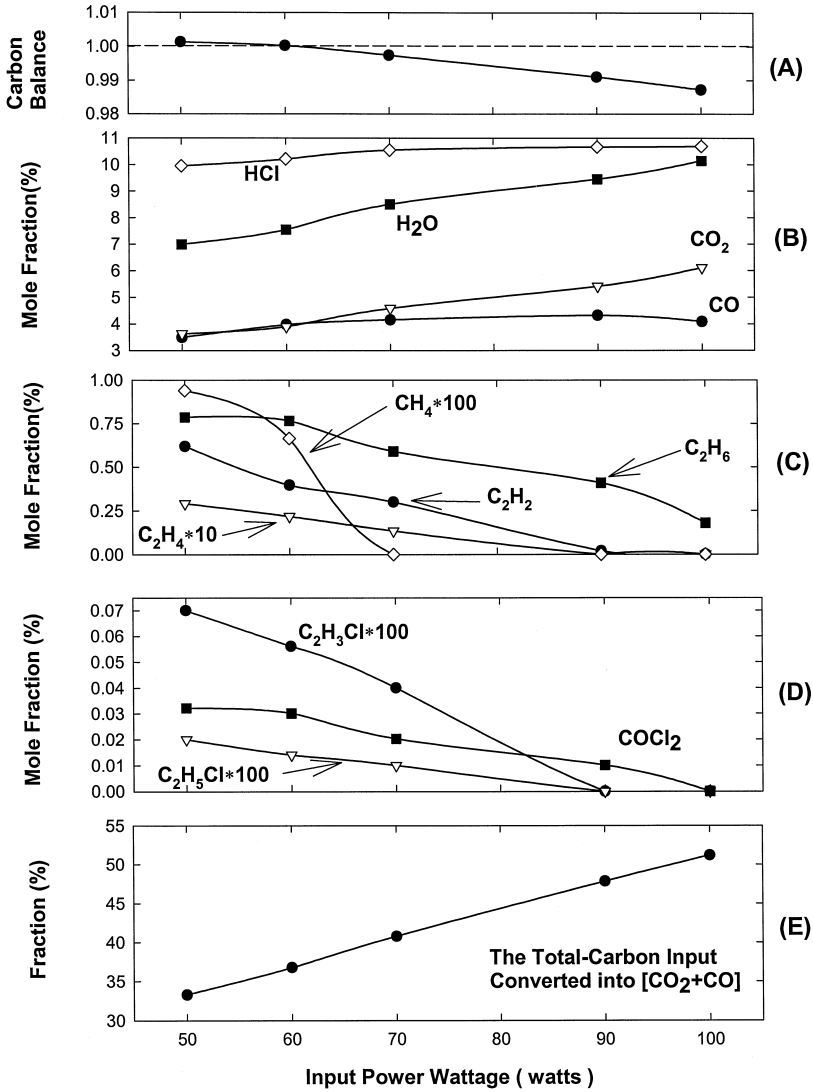

Fig. 4. The effect of input power wattage for carbon balance (A), effluent concentration of products (B ~ D), and the fraction of total-carbon converted into CO_2 and CO (E).

when the input power wattages were higher than 90 W. Due to the fact that more methyl chloride was converted into CO_2 and CO and the reaction pathway for $COCl_2$ formation was hindered, the effluent $COCl_2$ concentration was decreased by increasing the input power wattage [23]. As the input power wattage up to 100 W in the plasma reactor, the $COCl_2$ formation was hindered completely (Fig. 4D). These results reveal that more energy in the plasma reactor will result in the formation of more stable 'final products'

like CO_2, HCl and H_2O and enhance the decomposition of unstable species like $COCl_2$ [21].

As seen in Fig. 4(E), it is apparent that raising the input power wattages from 50 to 100 W resulted in an increase in the fraction of total-carbon input converted into $[CO_2 + CO]$ from 33.3% to 51.2% linearly. Higher input wattage provided more energy for the ionization of gas molecules, increased the effective collision frequency among the reactants, excited the Ar ($Ar*$) and free electrons (e^-), and therefore, elevated the fraction of total carbon input converted into CO_2 and CO.

3.4. Effect of CH_3Cl feeding concentration

In this investigation, argon was used as the carrier gas; the CH_3Cl feeding concentration were varied from 3% to 20%; the input power wattage was 50 W; the operational pressure was controlled at 20 Torr; the total gas flow rate was 100 sccm; and the equivalence ratio (ϕ) was 1.0.

At higher CH_3Cl feeding concentration, more soot formation and the polymerization were also found in the plasma reactor. This also resulted in a lower carbon balance in the effluent gas stream (Fig. 5A).

As shown in Fig. 5B, the mole fraction profiles for all species have the same increasing tend when the CH_3Cl feeding concentration was increased from 3% to 20%. In Fig. 5C, increases in CH_3Cl feeding concentration have increased the effluent concentration of CH_4, C_2H_2, C_2H_4, and C_2H_6. Similarly, increases in CH_3Cl feeding concentration have increased the levels of C_2H_3Cl, C_2H_5Cl, and $COCl_2$ (see Fig. 5D). These results are explained in terms of a higher possibility for hydrocarbon or chlorinated hydrocarbon formation due to the more abundant C and Cl sources arising from higher feeding of CH_3Cl.

Fig. 5E shows that when feeding CH_3Cl concentrations were increased from 3.0% to 20.0%, the fraction of the total-carbon input converted into $[CO_2 + CO]$ was decreased from 37.3% to 29.8%. As the equivalence ratio ($\phi = 1.0$) remained constant, the increasing of CH_3Cl concentration decreased the relative concentration of argon. In the plasma reactor, argon used for the carrier gas also acted as the energy transfer medium. The lower concentration of Ar in the feeding gas mixtures results in a lower concentration of excited $Ar*$ in the plasma reactor, and therefore, in a decreased CH_3Cl collision frequency and a reduction of the fraction of the total-carbon input converted into CO_2 and CO.

In conjunction with the foregoing discussion, the detailed reaction channels associated with the decomposition of CH_3Cl in the RF plasma reactor are presented in Fig. 6. In this figure arrows with varying line thicknesses are used as a visual guide to illustrate the relative importance of reaction pathways. It must be done with care, as under different set of conditions different reactions are likely to be important in affecting the product distributions.

3.5. Temperature profile in different operational conditions

In the plasma reactor, T (°C) is defined as the temperature measured at the exit of plasma reaction zone. The T (°C) of $CH_3Cl/O_2/Ar$ plasma was primarily affected by

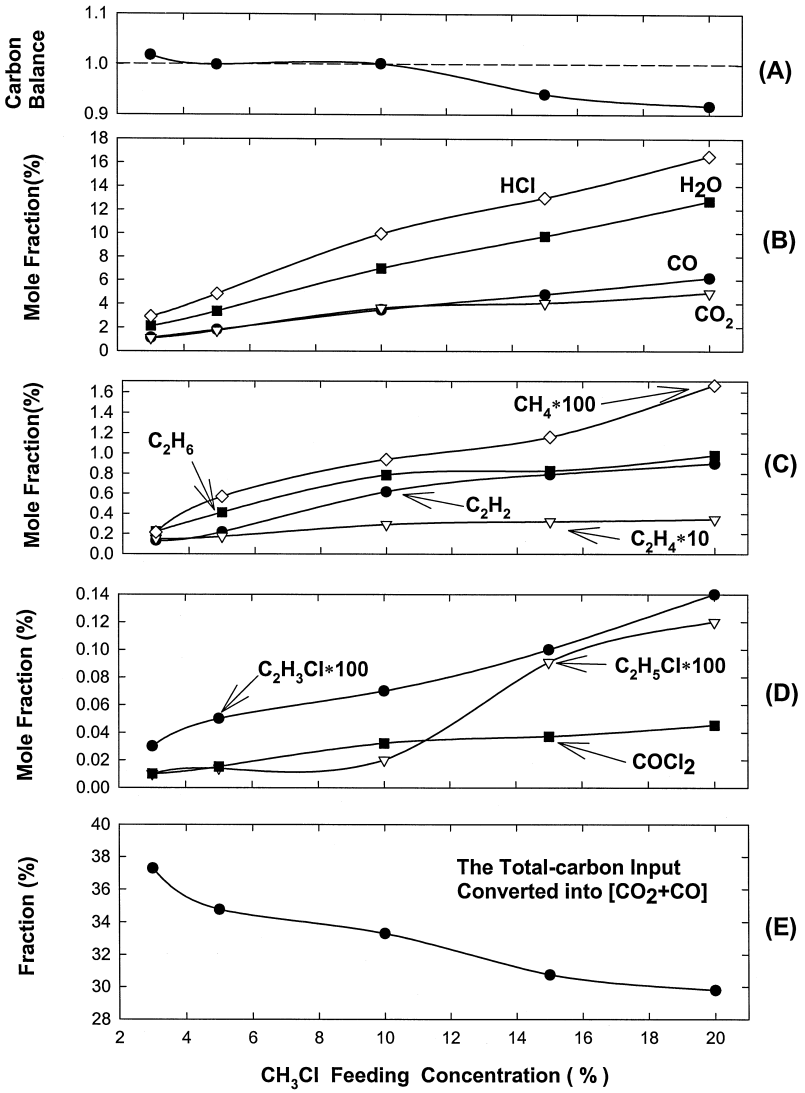

Fig. 5. The effect of CH_3Cl feeding concentration for carbon balance (A), effluent concentration of products (B ~ D), and the fraction of total-carbon converted into CO_2 and CO (E).

the input power wattage. The T (°C) were also under the influence of both the equivalence ratio and the CH_3Cl concentration in the feeding gas mixtures.

The T (°C) profiles of $CH_3Cl/O_2/Ar$ plasma at varied equivalence ratios, different input power wattages, and different CH_3Cl feeding concentrations are shown in Fig. 7. In this investigation, all T (°C) curves leveled off after 20 min from the time of starting the plasma generator. It can be seen in the Fig. 7 that the T (°C) curves are dominated by the input power wattage. Higher input power wattage provided more energy for the

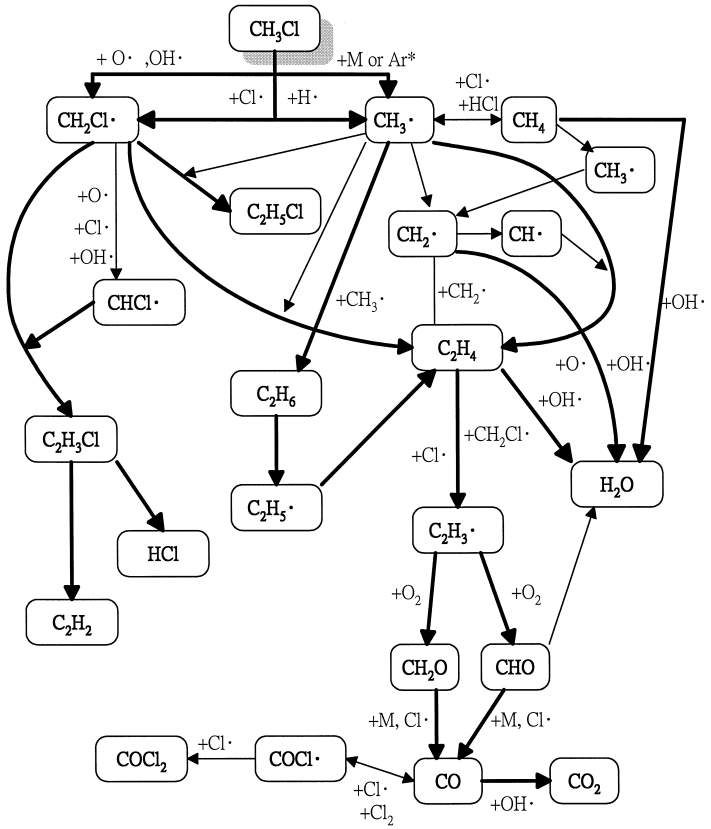

Fig. 6. Detailed reaction pathways for the decomposition of CH_3Cl in the RF plasma reactor.

ionization of gas molecules, increased the effective collision frequency among the reactants, excited the Ar (Ar$*$), and free electrons (e^-), and therefore, strongly elevated the T (°C) at different operational conditions.

According to the input power wattage, three ranges which covered all T (°C) could be found in this investigation. When the input power wattages were controlled at 90, 70, and 50 W, the T (°C) ranged from 340°C to 440°C, from 170°C to 330°C, and from 140°C to 260°C, respectively.

3.6. Mathematical model statement

Mathematical model can provide valuable information on the link existing between the various operating parameters and the methyl chloride decomposition efficiency. It is important to assess the dependence of the computed decomposition efficiency with respect to the wide range of parameters needed to describe the physical and chemical

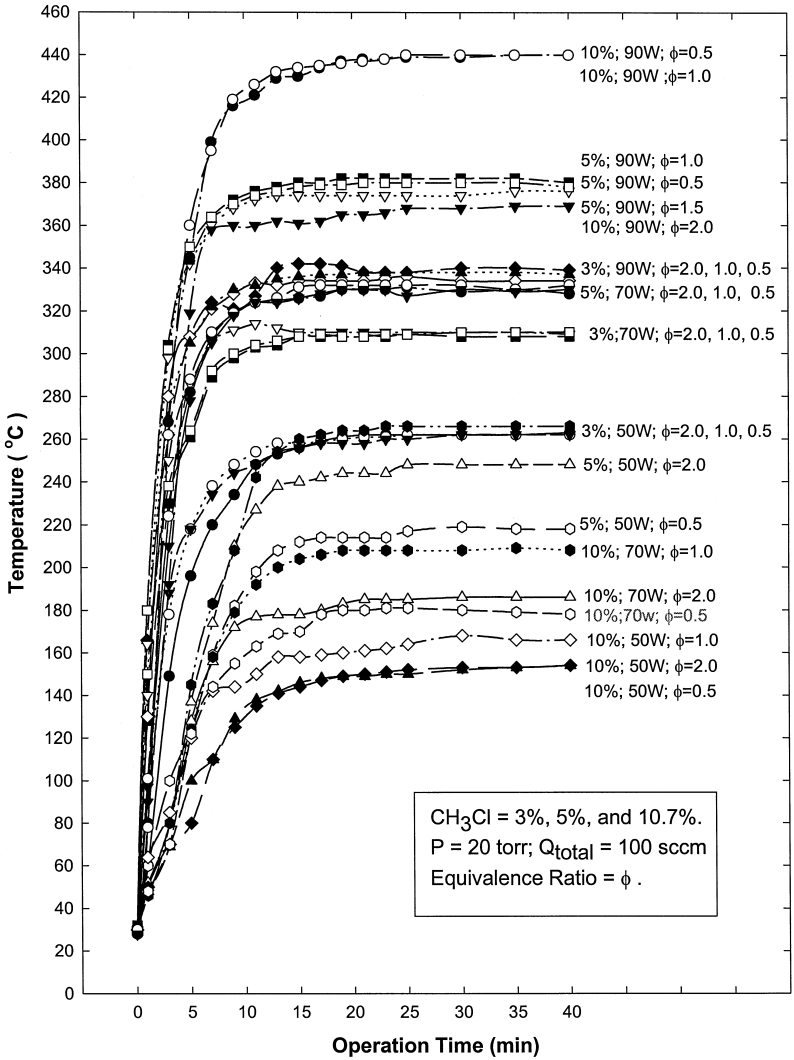

Fig. 7. Temperature profiles of CH_3Cl mixing with oxygen at different equivalence ratio value (ϕ) at different input power wattage.

processes involved. Then, statistical experimental design and analysis provide an optimal method to discover the relationship between a response and one or more control variables. If y is a response (i.e. decomposition fraction or efficiency) and X_1, X_2, $X_3, \ldots$ are a set of control variables (i.e. input power wattage, methyl chloride feeding concentration, equivalence ratio, etc.), then one can propose a functional relationship between the two:

$$y = f(X_1, X_2, X_3, \cdot) \tag{59}$$

Three operational parameters (as above mentioned) were selected to describe the performances in the reactor. For convenience, three operational parameters are abbreviated as following:

W = input power wattage (Watt);

C_{CH3Cl} = feeding concentration of CH_3Cl (vol/vol; %);

ϕ = equivalence ratio;

When the modeling are derived, the W, C_{CH3Cl}, and ϕ are the independent variables (or explanatory variables); the T (°C) or the η_{CH3Cl} is the dependent variable (or explained variable). In the feasible range, by means of controlling the independent variables at designed condition, the dependent variables can be obtained in the experiments. Then, the relationship between η_{CH3Cl} or T (°C) and those three operational parameters (i.e. W, C_{CH3Cl}, and ϕ) should be linked.

It is assumed that the T (°C) or the degree of CH_3Cl decomposition is the function of W, C_{CH3Cl}, and ϕ. That is,

$$T(°C) \propto f_1(W, C_{CH3Cl}, \phi) \tag{60}$$

$$\eta_{CH3Cl} \propto f_2(W, C_{CH3Cl}, \phi) \tag{61}$$

where$T$ (°C) = The temperature measured at the exit of plasma reaction zone in the plasma reactor, °C; η_{CH3Cl} = the decomposition fraction of CH_3Cl, %.

To correlate the dependent variables (or explained variables) with independent variable (or explanatory variable), the constants K_1 and K_2 are introduced. Therefore, we can obtain

$$T(°C) = K_1[W]^{X_1}[C_{CH3Cl}]^{Y_1}[\phi]^{Z_1} \tag{62}$$

$$\eta_{CH3Cl}(\%) = K_2[W]^{X_2}[C_{CH3Cl}]^{Y_2}[\phi]^{Z_2} \tag{63}$$

where Ki, Xi, Yi, and Zi ($i = 1 \sim 2$) are defined in Nomenclature. The constant K_1 has the unit which depends on the equation. That is,

$$K_1 \equiv [°C][\text{watt}]^{-X1} \tag{64}$$

Because η_{CH3Cl} is dimensionless number, the constant K_2 has the unit which depends on the equation. That is,

$$K_2 \equiv [\text{watt}]^{-X_2} \tag{65}$$

The unit for K_2 can be obtained after the X_2 is known.

Then, by taking natural log on both sides of Eqs. (46) and (47), we could obtain Eqs. (57) and (58) as follows:

$$\ln[T] = \ln[K_1] + X_1 \times \ln[W] + Y_1 \times \ln[C] + Z_1 \times \ln[\phi] \tag{66}$$

$$\ln[\eta_{CH3Cl}] = \ln[K_2] + X_2 \times \ln[W] + Y_2 \times \ln[C] + Z_2 \times \ln[\phi] \tag{67}$$

Based on the regression analysis, we can use the method of multiple regression to obtain the constants for K_1, X_1, Y_1, and Z_1 in Eq. (50) or the constants for K_2, X_2, Y_2, and Z_2 in Eq. (51). Consequently, we have

$$T(°C) = 2.9882[W]^{0.92357}[C_{CH3Cl}]^{-0.21967}[\phi]^{0.02757} \tag{68}$$

with an $R^2 = 0.676$; and

$$\eta_{CH3Cl}(\%) = 63.01[W]^{0.09186}[C_{CH3Cl}]^{-0.01499}[\phi]^{-0.00305} \quad (69)$$

with an $R^2 = 0.801$.

Using the expressions of η_{CH3Cl}, the prediction can be achieved within moderate conditions. In addition, the prediction of η_{CH3Cl} is better than that of T (°C).

3.6.1. Model sensitivity analysis

The aim of model sensitivity analysis was to gain more insight into the relative importance of the various operational parameters for the plasma reactor. The sensitivity of this model to change in each of three model parameters (i.e. W, C_{CH3Cl}, and ϕ) has been tested and some results are shown on Figs. 8 and 9. When the sensitivity of T (°C) in the plasma reactor or the sensitivity of CH_3Cl decomposition fraction are discussed, only one model parameter is changed from $+10\%$ increment to -10% reduction and all the others are fixed at initial values. Each individual sensitivity analysis for the T (°C) and η_{CH3Cl} is simulated from the initial values of $W = 50$ W, $C_{CH3Cl} = 3\%$ and $\phi = 1.0$ under the condition of $P = 20$ Torr and $Q = 100$ sccm. In Figs. 8 and 9, it is important to note that we define λ, $\Delta\lambda$, S, ΔS, $\Delta\lambda/\lambda$ and $\Delta S/S$, as follows:

$\lambda \equiv$ The initial value of each operational parameter (W, C_{CH3Cl} and ϕ, respectively), in processing Sensitivity Analysis.

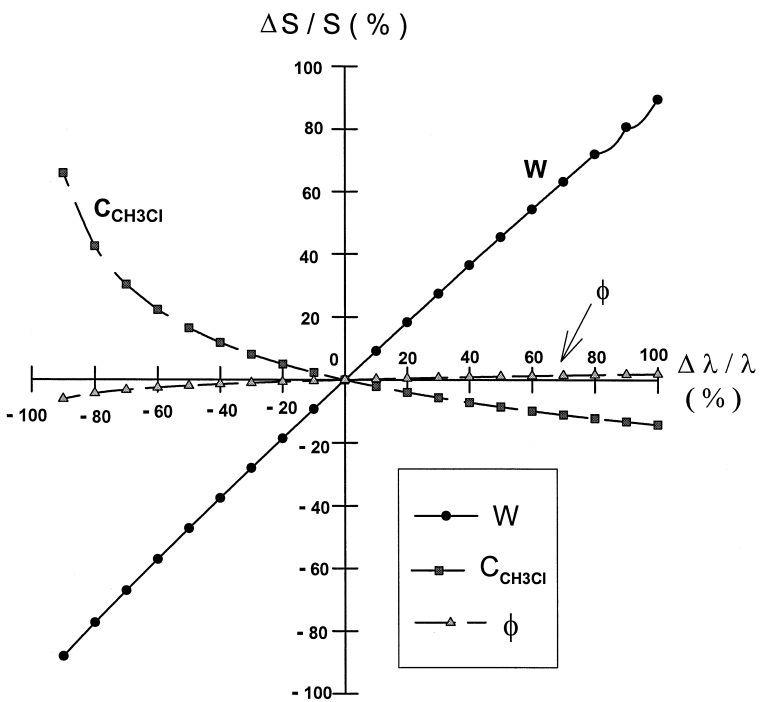

Fig. 8. The sensitivity of operational parameters on the temperature in the plasma reactor.

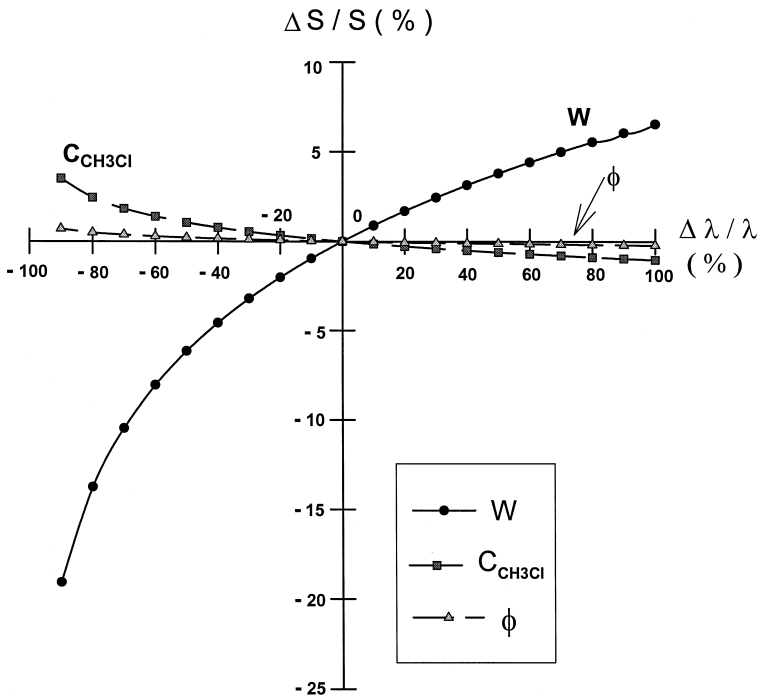

Fig. 9. The sensitivity of operational parameters on the CH_3Cl decomposition fraction (%) in the plasma reactor.

$\Delta\lambda \equiv$ For each operational parameter (W, C_{CH3Cl} and ϕ, respectively), the amount of increase or reduction, in processing Sensitivity Analysis.
$S \equiv$ The initial predicted value of η_{CH3Cl} (%) or T (°C) from the certain value of each operational parameter (W, C_{CH3Cl} and ϕ), respectively.
$\Delta S \equiv$ The changes (%) of η_{CH3Cl} (%) or T (°C) for each operational parameter (W, C_{CH3Cl} and ϕ), respectively.
$\Delta\lambda/\lambda \equiv$ For each operational parameter (W, C_{CH3Cl} and ϕ), respectively, the amount of increase or reduction divided by the initial value, in processing Sensitivity Analysis.
$\Delta S/S \equiv$ The changes (%) of η_{CH3Cl} (%) or T (°C) for each operational parameter (W, C_{CH3Cl} and ϕ, respectively) standardized by the initial predicted value, respectively.

3.6.2. Sensitivity for the T (°C) in the plasma reactor

For the effects of the feeding concentration of CH_3Cl on T (°C) (Fig. 8), the $\Delta S/S$ increases sharply from 0% to 65.8% with the $\Delta\lambda/\lambda$ changed from 0% to -90%, but $\Delta S/S$ decreases seems moderate from 0% to -14.1% with the $\Delta\lambda/\lambda$ changed from 0% to $+100$%. Therefore, the change of CH_3Cl feeding concentration has a significant effect on the T (°C) in the plasma reactor, especially for the dilution condition. This indicates that the lower feeding concentration of CH_3Cl is of benefit to control the T (°C) within the moderate operational conditions.

In Fig. 8, the sensitivity analysis also indicates that either increasing or decreasing the input power wattage has a significant effect on the T (°C) in the plasma reactor. When the $\Delta\lambda/\lambda$ was changed from -90% to 100%, the $\Delta S/S$ responded from -88.1% to 89.7%, which leads to the relative 176.8% difference. This means that W is an important parameter in governing the T (°C) in the plasma reactor because the plasma reaction is associated mainly with the energy provided.

The tendency of ϕ in Fig. 8 is different from that of W or C_{CH3Cl}, the ϕ is less sensitive than that of W or C_{CH3Cl}. For the change of ϕ, when the $\Delta\lambda/\lambda$ was changed from -90% to 100%, the $\Delta S/S$ responded only from -6.2% to 1.9%. To be brief, the significance of sensitivity for the T (°C) in the plasma reactor is: $W > C_{CH3Cl} > \phi$.

3.6.3. Sensitivity for the decomposition fraction of CH_3Cl

For the effects of the model parameters (i.e. W, C_{CH3Cl}, and ϕ) on η_{CH3Cl}, the whole tendency of Fig. 9 is more gentle than that of Fig. 8. As far as the change of W, C_{CH3Cl}, and ϕ is concerned, as the $\Delta\lambda/\lambda$ was changed from -90% to 100%, the $\Delta S/S$ responded from -19.1% to 6.6%, from 3.5% to -1.0%, and from 0.7% to -0.2%, for W, C_{CH3Cl}, and ϕ, respectively. This shows that W has greater effect on η_{CH3Cl} than on C_{CH3Cl} and ϕ. Generally, the significance of sensitivity for η_{CH3Cl} is: $W > C_{CH3Cl} > \phi$.

4. Conclusions

(1) In the $CH_3Cl/O_2/Ar$ plasma, the decomposition fraction of CH_3Cl was over 99.99%, which occurred around 440°C in the condition designed for 3% of CH_3Cl feeding concentration, 1.0 of equivalence ratio (ϕ), 20 Torr of operation pressure, 100 sccm of total gas flow rate and 100 watts of input power wattage.

(2) In this plasma reactor, the CH_3Cl decomposition fractions increase when the equivalence ratio is raised to values around or below stoichiometry; and then decrease either sharply (50 W) or moderately (70 W) when the equivalence ratio goes up or down to values exceeding stoichiometry. However, there is no significant difference for those in higher input power wattages (both 90 and 100 W).

(3) At higher ϕ values, higher CH_3Cl feeding concentrations, and higher input power wattages, more soot formation and polymerization were also found in the plasma reactor. These resulted in a lower carbon balance in the effluent gas stream.

(4) Both methyl chloride decomposition efficiency and fraction of total-carbon input converted into CO and CO_2 were decreased by increasing the methyl chloride feeding concentration.

(5) Higher input power wattage can increase both CH_3Cl decomposition fraction and the fraction of total-carbon input converted into CO and CO_2 and decrease the effluent concentration of $COCl_2$. As the input power wattage increased up to 100 Watt in the plasma reactor, the $COCl_2$ formation was hindered completely.

(6) Input power wattage (W) is the most important parameter in governing the temperature in the plasma reactor because the plasma reaction is associated mainly with the energy provided. To be brief, the significance of sensitivity for the T (°C) in the plasma reactor is: $W > C_{CH3Cl} > \phi$.

(7) This study shows that W has greater effect on η_{CH3Cl} than on C_{CH3Cl} and ϕ. Generally, the significance of sensitivity for η_{CH3Cl} is: $W > C_{CH3Cl} > \phi$.

Nomenclature

C_{CH3Cl}	Feeding concentration of CH_3Cl (vol/vol, %)
P	Operational pressure in the RF plasma reactor (Torr)
Q	Total gas flow rate (sccm, $cm^3\ min^{-1}$ at 0°C and 1 atm)
W	Input power wattage (Watt)
η_{CH3Cl}	Decomposition fraction of CH_3Cl (%)
T (°C)	The temperature measured at the exit of plasma reaction zone in the plasma reactor (°C)
K_1	Constant of mathematical model, which links the temperature in the plasma reactor (°C) and operational parameters.
X_1	Constant of power factor in the mathematical model of T for the item of $[W]$.
Y_1	Constant of power factor in the mathematical model of T for the item of $[C_{CH3Cl}]$.
Z_1	Constant of power factor in the mathematical model of T for the item of $[\phi]$.
K_2	Constant of mathematical model, which links CH_3Cl decomposition fraction and operational parameters.
X_2	Constant of power factor in the mathematical model of η_{CH3Cl} for the item of $[W]$.
Y_2	Constant of power factor in the mathematical model of η_{CH3Cl} for the item of $[C_{CH3Cl}]$.
Z_2	Constant of power factor in the mathematical model of η_{CH3Cl} for the item of $[\phi]$.
$\Delta S/S$	The changes (%) of η_{CH3Cl} (%) or T (°C) for each operational parameter (W, C_{CH3Cl} and ϕ, respectively) standardized by the initial predicted value, respectively.
$\Delta\lambda/\lambda$	For each operational parameter (W, C_{CH3Cl} and ϕ, respectively), the amount of increase or reduction divided by the initial value, in processing Sensitivity Analysis.

Acknowledgements

This research was supported, in part, by the National Science Council, Taiwan, grant No. NSC-87-2218-E006-067.

References

[1] C.P. Koshland, S. Lee, D. Lucas, Combust. Flame 92 (1993) 106.
[2] S. Sstyapal, J.H. Werner, T.A. Cool, Combust. Sci. Technol. 106 (1995) 229.
[3] W. Ho, M.R. Booty, R.S. Magee, J.W. Bozzelli, Ind. Eng. Chem. Res. 34 (1995) 4185.
[4] R. Yildirim, S.M. Senkan, Ind. Eng. Chem. Res. 32 (1993) 438.
[5] S.B. Karra, S.M. Senkan, Ind. Eng. Chem. Res. 27 (1988) 1163.
[6] K.C. McGee, M.D. Driessen, V.H. Grassian, J. Catal. 159 (1996) 69.
[7] Y. Sun, S.M. Campbell, J.H. Lunford, G.E. Lewis, D. Palke, L. Tau, J. Catal. 143 (1993) 32.
[8] W. Ho, R.B. Barat, J.W. Bozzelli, Combust. Flame 88 (1992) 265.
[9] J. Tavakoli, H.M. Chiang, J.W. Bozzelli, Combust. Sci. Technol. 101 (1994) 135.
[10] R.B. Barat, J.W. Bozzelli, J. Phys. Chem. 96 (1992) 2494.
[11] E.W. Kaiser, T.J. Wallington, J. Phys. Chem. 98 (1994) 5679.
[12] Y. Shen, Y. Ku, J. Hazard. Materials 54 (1997) 189.
[13] D.M. Pearl, P.D. Burrow, Chem. Phys. Letters 206 (1993) 483.
[14] C. Vinckier, I. Vanhees, D. Sengupta, M.T. Nguyen, J. Phys. Chem. 100 (1996) 8302.
[15] R.B. Barat, J.W. Bozzelli, Environ. Sci. Technol. 23 (1989) 666.
[16] T. Yamamoto, B.R. Locke, W.C. Finney, G. Saithamoorthy, S. Goldstein, R.C. Clark, Proceedings of the First Asia-Pacific International Symposium on the Basic and Application of Plasma Technology, Dec. 15–16, 1997, p. 161.
[17] T.A. Cleland, D.W. Hess, Plasma Chem. Plasma Process. 7 (1987) 370.
[18] J. Arno, J.W. Bevan, M. Moisan, Environ. Sci. Technol. 29 (1995) 1961.
[19] J. Arno, J.W. Bevan, M. Moisan, Environ. Sci. Technol. 30 (1996) 2427.
[20] J.S. Chang, Proceedings of the First Asia-Pacific International Symposium on the Basic and Application of Plasma Technology, Dec. 15–16, 1997, p. 11.
[21] C.T. Li, W.J. Lee, C.Y. Chen, T. Wang, J. of Chem. Technol. Biotechnol. 66 (1996) 382.
[22] L.T. Hsieh, W.J. Lee, C.Y. Chen, M.B. Chang, H.C. Chang, Plasma Chem. Plasma Process. 18 (1998) 215.
[23] W.J. Lee, C.Y. Chen, W.C. Lin, Y.T. Wang, C.J. Chin, J. Hazard. Materials 48 (1996) 51.
[24] P. Vaughan, T. Lindahl, B. Sedgwick, Mutation Res., DNA Repair 293 (1993) 249.
[25] L.T. Hsieh, 'Reaction Mechanism of Carbon Dioxide and Methane in an RF Plasma Reactor', Ph.D. Dissertation, Department of Environmental Engineering, National Cheng Kung University, Taiwan, June 1998.